Design optimization of an engine air intake

N. Hoyle*, N.W. Bressloff, A.J. Keane

University of Southampton, Southampton SO17 1BJ, UK

Abstract

A novel geometry modeling technique is defined for the optimization of pressure recovery through a two-dimensional subsonic diffuser based on that of an F1 race car airbox. The airbox design procedure involves considering the expansion of the air entering the airbox coupled with a bend through 90°, both of which are discussed separately before uniting the two in a final optimization study. The geometry modeling technique discussed allows for potentially radical designs with high pressure recoveries.

Keywords: Diffuser; Computational fluid dynamics (CFD); Geometry Modeling; Shape optimization

1. Introduction

Engine air intake design is an important process within both the automotive and aerospace industries. When designing such intakes, the aim for the internal flow is to ensure that the engine can be provided with as great an increase of static pressure at the engine face as possible.

For this reason, diffusers are commonly used to provide an efficient reduction in flow velocity to convert a large fraction of the dynamic pressure at diffuser entry, into static pressure at its exit, i.e. at the engine face.

The engine airbox on an F1 race car is an interesting challenge as it requires both a large expansion and a turn of the flow through 90° within a very short distance, prescribed by the engine layout configuration and roll structure specifications.

Currently, F1 teams use a configuration which places a 3-litre V10 engine behind the driver (see Fig. 1) with the airbox positioned inside the roll-bar thus taking advantage of the ramming effects of the oncoming air at high speeds. An increase in the static pressure available to the flow into the engine on its intake stroke increases the cylinder charge density and hence engine power.

In F1 cars, the exit of the diffuser sits over an offset array of ten intake trumpets. Because of this, uniformity of pressure here is also important.

In this study, we have initially considered the two main features of the diffuser separately: that of expanding the flow and that of turning the flow. Much research has been carried out for the case of straight, two-dimensional diffusers. Practical experimentation has been used to classify the major flow regimes within these diffusers [1,2]. Relations between the flow regimes and the geometry were discovered by Reneau et al. [3] and, at the same time, studies into the manipulation of the wall geometry to create more efficient designs were investigated [4].

Here, we first find a suitable method for parameterizing the geometry of a diffuser with no bend, followed by a bend with no expansion. The expansion and bend are then fused together and an optimization procedure employed to develop the design further.

2. Objective

Our objective is maximizing pressure recovery solely from the internal flow. In this case we assume steady, one-dimensional, incompressible inlet flow so that the pressure recovery, C_p, may be defined as

$$C_p = \frac{p_e - p_u}{q_u} \tag{1}$$

where p_e and p_u are the mass-averaged static pressure values at the exit and upstream locations, respectively, and

$$q_u = \frac{1}{2}\rho U^2 \tag{2}$$

*Corresponding author. Tel.: +44 2380 595194; Fax: +44 2380 594813; E-mail: nici@soton.ac.uk

Computational Fluid and Solid Mechanics 2005
K.J. Bathe (Editor)

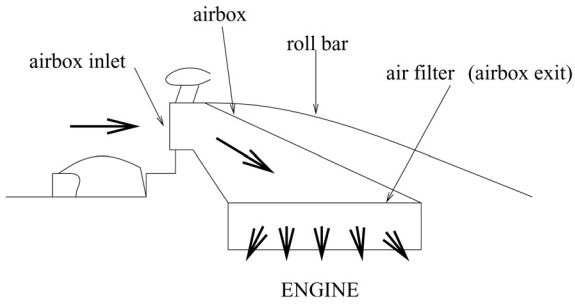

Fig. 1. Airbox positioning within the F1 car.

denotes the dynamic pressure, ρ being the density and U the mass-averaged inlet velocity.

3. Geometry parameterization

3.1. Straight diffuser

Early work on wall contouring for a straight two-dimensional diffuser [4] was based on a wall geometry defined by just one parameter. A bell-shaped optimal wall contour was found. Madsen et al. [5] brought in the use of CFD and modern optimizer codes using a B-spline parameterization with five master points along the wall.

For our F1 case, however, the expansion ratio is much larger combined with a shorter diffuser length than those tested by Carlson et al. or Madsen et al. Consequently, three different geometric parameterizations of the wall were tested here to obtain an idea as to how the flow responds in these conditions and how much local wall control is possible. First, a set of four cubic splines joined together to form one piece-wise cubic spline passing through five points with five design variables. Point one is fixed at the entry position, point two has its x and y coordinates variable, point three has its x coordinate fixed at half the centerline length and its y coordinate variable, point four has both its x and y coordinates variable and point five is fixed at the exit position. Second, a single Hicks–Henne bump function [6,7] with three design variables, namely, amplitude, x location of bump and bump width. And finally, a double Hicks–Henne bump function with six design variables.

3.2. An elbow turning through 90°

Two parameterizations were tested for modeling the centerline of the diffuser using a constant width duct which turns through 90°. One method employed piece-wise splines passing through three points along the centerline and the second a Bezier curve with three control points.

3.3. The airbox design

Methods from the preceding two sections were next fused together to create a two-dimensional airbox model. Hence, our model was split into three separate uncoupled sections; the centerline bend, the upper wall, and the lower wall. This decoupling maximizes the amount of local control given to the optimizer and allows the production of potentially radical results.

The initial upper wall shape was taken as the optimum shape from the straight diffuser study. The centerline was then bent round according to the best results from the turning elbow study with the three control points defining the bend by CP1(x,y), CP2(x,y) and CP3(x,y), see Fig. 2. The equivalent x values of the straight diffuser on the upper wall were measured as a ratio along the centerline with the equivalent y values (r_{u1}, r_{u2}, r_{u3}) measured normal to the centerline. With the same method, the lower wall would tend to fold in on itself and gain loops. To avoid this, we used the angles θ_1, θ_2

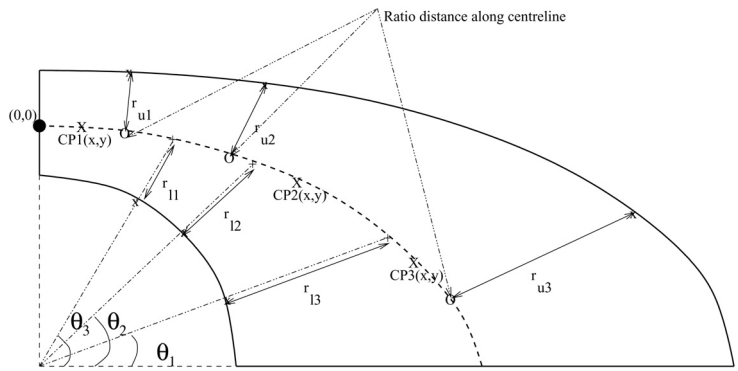

Fig. 2. Geometry parameterization of airbox.

and θ_3, with θ_2 fixed at 45°, to obtain lines intersecting with the centerline. The distances r_{l1}, r_{l2} and r_{l3} could be then measured along these lines.

4. CFD analysis and optimization study

The characteristic strategy when considering an optimization loop is outlined in the steps below:

(1) Specify a parametric geometry.
(2) Construct inputs using a Design of Experiments (DoE) approach.
(3) Run CFD simulations.
(4) Build a response surface model (RSM).
(5) Evaluate RSM. If modifications are necessary, repeat steps (4) and (5).
(6) Population and gradient-based search methods using RSM.
(7) Further CFD evaluations.
(8) OK? If more update design points are necessary, repeat steps (4) to (7).
(9) Result: optimum design.

Our geometry is built using a CAD engine and then imported into a meshing tool. Before optimization, an appropriate mesh resolution was found for sufficient accuracy and convergence of the solution in FLUENT. With a fixed mass flow rate at the inlet, equivalent to a velocity of approximately 70 m/s, a paved quad structure of a 30K cell mesh was chosen.

An initial 25 point DoE search using an LPτ method was implemented for each optimization process. Sequential update points are then added to build up the RSM *apropos* achieving an optimum pressure recovery between the exit and the entry. This response surface is built by optimizing the expected improvement available due to a kriging process using the OPTIONS Design Exploration System [8]. This particular loop is preferential to avoid the points becoming trapped in a local maximum of the response surface. For further details on efficient optimization processes, see Jones [9].

The CFD evaluations were carried out via two-dimensional steady Reynolds-averaged Navier–Stokes equations employing the standard k-ϵ turbulence model.

Following the initial DoE search, 75 update points were sequentially added to the response surface to obtain the optimum design.

5. Results

5.1. Straight diffuser

In this case the optimum shapes from all three parameterizations were not bell-shaped. If the air was expanded quickly at the start of the diffuser, at our set speed, the boundary layer was not sufficiently energized to remain attached. Interestingly, all three optima showed a geometry converging slightly at the inlet and expanding linearly after that, as can be seen in Fig. 3. The slight convergence accelerates the flow sufficiently to increase the turbulence of the flow which, in turn, increases the turbulence of the boundary layer hence preventing the onset of separation. This convergent–divergent diffuser returns a slightly higher pressure recovery than that of the straight wall. Additionally, the pressure distortion over the exit for the optimum design is reduced.

5.2. An elbow turning through 90°

This study demonstrated that piecewise splines provide slightly more local control along the bend than the Bezier curve. This is primarily due to the Bezier curve requiring extra control points positioned at either end to ensure tangency conditions.

5.3. The airbox design

Even with a relatively large number of design variables, the optimization process worked well and its development is plotted in Fig. 4. Design points which returned a pressure recovery lower than $C_p = 0.65$ were

Fig. 3. Streamlines illustrating the flow field in a straight wall (left) and optimum wall (right) diffuser.

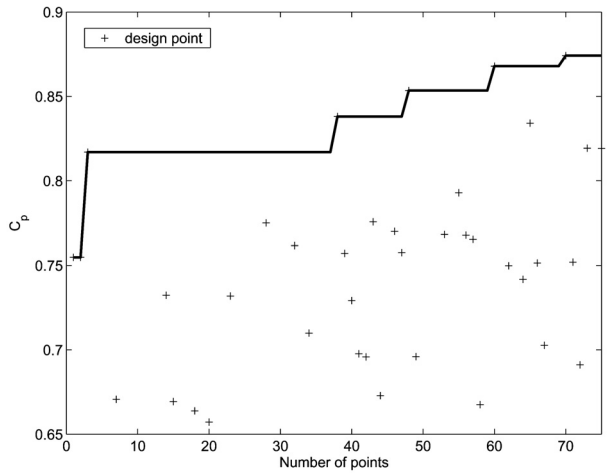

Fig. 4. Optimization history.

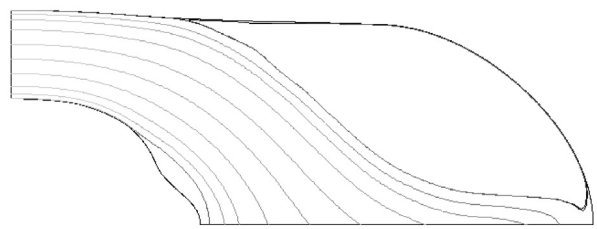

Fig. 5. Streamlines illustrating the flow field in the optimum design.

trimmed off the figure. The bold line indicates the current best optimum as each update point was added. Our optimum design can be seen in Fig. 5. Interestingly, a large bulb has formed along the upper wall and a smaller bulb can be seen on the lower wall. Both have the effect of catching the bubble of separated flow allowing the main core of the flow to follow a path akin to the shape of a more intuitively shaped diffuser.

6. Conclusion

We have observed that by uncoupling the walls and centerline of a curved diffuser we can produce radical results. The resulting geometry has an extended bulb on the rear of the diffuser and a smaller bulb on the lower front wall. By capturing and containing the separation bubbles occurring in the airbox within these bulbs we can obtain a high pressure recovery and allow a uniform pressure distribution over the filter.

References

[1] Kline SJ, Abbott DE, Fox RW. Optimum design of straight-walled diffusers. Journal of Basic Engineering, Trans. ASME, Series D 1959;81:321–331.
[2] Fox RW, Kline SJ. Flow regimes in curved subsonic diffusers. Journal of Basic Engineering, Trans. ASME, Series D 1962;84:303–316.
[3] Reneau LR, Johnston JP, Kline SJ. Performance and design of straight, two-dimensional diffusers. Journal of Basic Engineering, 1967;March:141–150.

[4] Carlson JJ, Johnston JP, Sagi CJ. Effects of wall shape on flow regimes and performance in straight two-dimensional diffusers. Journal of Basic Engineering, 1967;March:151–160.
[5] Madsen JI, Olhoff N, Condra TJ. Proc 3rd World Congress on Structural and Multidisciplinary Optimization, Buffalo, NY, USA, 17–21 May, 1999.
[6] Hicks RM, Henne PA. Wing design by numerical optimization. J Aircraft 1978;15(7):407–412.
[7] Sóbester AJ, Keane A. Empirical comparison of gradient-based methods on an engine-inlet shape optimization problem. AIAA 2002–5507.
[8] Keane AJ. The options design exploration system reference manual and user guide – version b3.1, http://www.soton.ac.uk/~ajk/options.ps, 2002.
[9] Jones DR. A taxonomy of global optimization methods based on response surfaces. J Global Optimization 2001;21:315–383.